FINITE ELEMENT ANALYSIS OF HIP IMPLANTS WITH ADDITIVE MANUFACTURED LATTICE INTERNAL GEOMETRY

Nikolaos Kladovasilakis[1], Konstantinos Tsongas[1], Panagiotis Kyratsis[2], Dimitrios Tzetzis[1]

[1] International Hellenic University, School of Science and Technology, Digital Manufacturing and Materials Characterisation Laboratory, 14km Thessaloniki - N. Moudania, 57001, Greece.
[2] University of Western Macedonia, Department of Product and Systems Design Engineering, Kila Kozani,50100, Greece.

Corresponding author: Dimitrios Tzetzis, d.tzetzis@ihu.edu.gr

Abstract: Additive manufacturing technology is widely applied to optimize products in several industries and more specifically in the field of biomechanical engineering. Currently, medical implants are made of solid metal to withstand the applied loads, however this leads to relative heavy-weight implants that cause difficulties in compatibility with bone tissues. This paper investigates the utility of lattice structures (cellular materials) for topology optimization on hip implants with Ti4Al6V as a construction material. Lattice structures are known for their complex geometries and advanced mechanical behaviour. Hip implants containing three different lattice structures are examined through finite element analysis (FEA) under *in vivo* loads. Consequently, the re-designed hip implants combine areas with solid material and regions with lattice structures. Results have shown that the topology optimization of hip implant geometry through lattice structures is functional and safe to use. The most suitable lattice structure was proposed in terms of stress behaviour.

Key words: Biomechanics, Computer Aided Design, Finite Element Analysis, Lattice Designs, Hip Implants.

1. INTRODUCTION

Recent developments in the fields of product design and manufacture have led to the improvement of the structure and the function of a fabricated part. Specifically, due to the development of additive manufacturing (AM), it is now possible to fabricate complex geometries, which are topologically optimized (Tyflopoulos et. al, 2018). Topology optimization (TO) is a procedure that, together with sizing optimization and shape optimization, completes the process of structural optimization (Bendsøe and Sigmund, 2003). Through the topology optimization, there is an improvement of the material's mass distribution within the defined external volume. The objective of this process is to maintain the desired mechanical properties of the part with the least possible mass (Ehrgott, 2005). There are two different approaches for the TO process, density-based and truss-based approach. The density-based approach is identical to generative design (Rosen, 2014). On the other hand, truss-based approach is based on the periodic creation of unit cells within the volume's domain (Larsen et. al., 2018). Nowadays, there is a plethora of applications in various industries that topologically optimize their products using one of the two above-mentioned approaches, indicatively in aeronautical industry (Gebisa and Lemu, 2017), automotive industry (Li et. al., 2015) and biomechanical industry (González-Henríquez et. al., 2019) etc.

In this study and in the biomechanical industry, for items such as implants and scaffolds, the truss-based approach is commonly used for their topological optimization. Specifically, within the volume of the product, selected solid regions are replaced by lattice structures with a specific unit cell geometry and relative density. Besides, the advantage of reducing the mass of the material, for the utility in biomechanical applications, this process has another important advantage, which is the facilitation of the tissue regeneration process, due to the high porosity and the high surface area to volume ratio of the lattice structures (Heinl et. al., 2008). There are numerous lattice structures, 2D lattice structures that refer to honeycombs, prismatic geometries (Mansour et. al., 2019) and 3D lattice structures that divided in two subcategories: strut-structures and sheet-structures (Helou and Kara et. al., 2018). The most common strut-structures are the octet and the skeletal triply periodic minimal surfaces (TPMS). On the other hand, most widespread lattice sheet-structures are the sheet-TPMS, namely Gyroid, Schwarz Diamond etc. According to Gibson and Ashby (1997), all lattice structures lead to degradation of the material's mechanical properties. The influence of the lattice structure on the mechanical behavior of a product depends mainly on the relative density and on the geometry of the applied lattice structure. Relative densities less than 60% activate the size effect, which has an increasing impact on mechanical performance

as the relative density is reduced. On the other hand, lattice structures that exhibit stretching-dominated behavior are less affected by the size effect compared to lattice structures that exhibit bending-dominated behaviour (Al-Ketan and Al-Rub, 2019). Therefore, Al Ketan et. al. (2018) proposes lattice structures that have stretching-dominated behavior for biomechanical applications which receive increased stresses, such as octet and sheet structures.

This article deals with orthopedic implants that contain lattice structures. In addition, there are several studies that have tried to combine AM technique with orthopedic implants through customization and lattice structures. Mahmoud and Elbestawi (2017) have gathered the majority of these studies in a comprehensive review, which summarizes the use of AM technologies to produce orthopedic implants from lattice structures and functionally graded materials. Gabbrielli et. al. (2006) and España et. al. (2010) investigate the possibility of using lattice structures in acetabular cup for mechanical and biological advantages. Moreover, Hazlehurst et al. (2013) suggested to manufacture hip implant that consists cubic lattice structures in whole internal body of the implant, this led to direct reduction of the implant's stiffness and its strength. Limmahakhun et al. (2017) and González et. al. (2016) researched innovation designs in order to optimize the utility of lattice in orthopedic implant and increase their mechanical strength, this was achieved by functionally gradation of the lattice structure.

This study, having gathered the majority of literature research on the use of lattice structures in orthopedic implants, proposes an innovative orthopedic hip implant design with advanced lattice structures in order to address the reduction in strength of these implants.

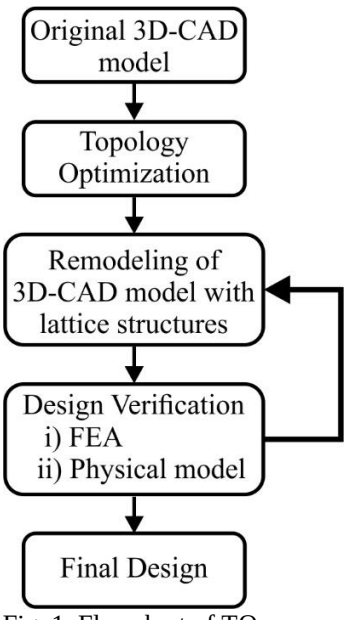

Fig. 1. Flowchart of TO process

Figure 1 portrays a flowchart of the topology optimization process via lattice structures depending on the mechanical behaviour. Specifically, at first a hip implant was designed according to international medical standards and then, through FEA, its mechanical behaviour was examined under in vivo static loads. Furthermore, specific regions of the implant are replaced by lattice structures that have been shown to exhibit stretching-dominated behaviour, those are octet strut-structure and gyroid, Schwarz diamond sheet-structures. Then, these three lattice structures are examined and evaluated for their mechanical performance under the same in vivo loads.

2. DESIGN AND FINITE ELEMENT ANALYSIS METHOD

2.1 Design of hip implant

The design of a hip implant obeys a series of international standards (ASTM F2033-12, 2012). In addition, there is extensive literature research that examines the different design approaches for this type of implant. A hip implant consists of three distinct regions: the head, the neck, and the rest of the body (stem). The basic design parameters from hip implant design are the head diameter, the diameter and length of the neck, the length of the intramedullary implant, the cross-section of the stem and the angle of placement of the head relative to the main body. Table 1 contains all these design parameters and their ranges.

Table 1. Ranges of hip implant's design parameters

Design parameters	Typical values
Head diameter	22mm – 45mm
Length of neck	10mm – 40mm
Neck diameter	13mm – 30mm
Length of intramedullary stem	120mm –180mm
Angle of head placement	135° – 145°

According to existing studies (Charnley et. al. 1969 and McKnee, 1967), the diameter of the head (ball) ranges between 22 mm to 45 mm. Moreover, the length and diameter of the neck range between 10 mm (short-neck) to 40 mm (long-neck) and 13mm to 30 mm, respectively (Müller, 1970 and Hybbinette, 1985). The length of the intramedullary stem of the implant ranges from 120 mm to 180 mm and the neck-shaft angle varies between 135° to 145° (El-Shiekh, 2002).

In order to study the topology optimization through lattice structures of an orthopedic hip implant, a new hip implant was designed that meets the above-mentioned standards. Furthermore, the designed hip implant for this study has the following characteristics. The intramedullary stem's length is 128 mm, while the neck's length is 35 mm. In addition, the diameter of the neck is 18 mm and the diameter of the head is 45 mm. The placement angle of the neck and head in relation

to the axis of the implant is 135° degrees and the angular range is almost 120° degrees. Figure 2 illustrates the design of hip implant, its basic dimensions and its cross-section.

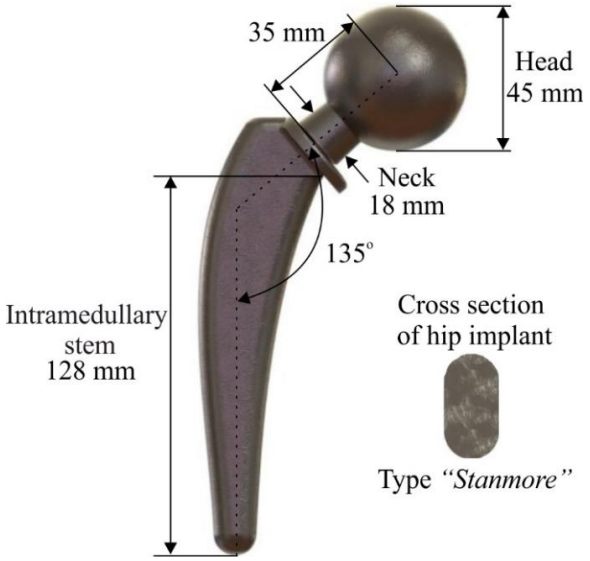

Fig. 2. Design of hip implant

2.2 Set-up of finite element analysis

This research has developed finite element models (FEM) of each hip implant design with different lattice structures, examined under static *in vivo* conditions in order to study their mechanical behavior. It is worth mentioning that FEA for each implant focuses mainly on the elastic behavior, the determination of yield point and the calculation of safety factor of the topologically optimized hip implants. ANSYS™ software was used for the finite element analysis and in particular static structural module was used to simulate the quasi-static loading. The mesh consisted of tetrahedrals elements for whole body of the implant and contained approximately 250,000 elements in total. For medical use and especially for orthopedic hip implants, the proposed material from the literature is the titanium alloy Ti6Al4V. In order to be suitable for this application titanium alloy should fulfill the international standards of UNS R56400 and ASTM B348 Grade 5 (ASTM B348 / B348M-19, 2019 and Boyer, 1994). Table 2, presents the mechanical properties of this titanium alloy which were used in order to build a model that simulate the material with combination of isotropic elasticity and bilinear isotropic hardening.

Table 2. Mechanical Properties of Ti6Al4V Grade 5

Mechanical properties	Typical values
Elastic Modulus	114 GPa
Poisson Ratio	0.342
Yield Strength	910 MPa
Ultimate Yield Strength	1100 MPa

Furthermore, in order to complete the FEMs, it is necessary to determine, based on the literature, the conditions for implant's support and the maximum loads that the implant receives from the human body under *in vivo* loading conditions. Hence, according to Ducheyne and Hasting (1984), the hip implant has fixed support at the bottom of its geometry in contact with the femur bone, without relying in to calcar support. Moreover, the received loads remain to be defined as to the point of application, the direction of the loading and the amount of forces. El-Shiekh (2002), who has carried out a comprehensive research in hip joint replacement under static and dynamic loading, had shown that the forces, caused by the human body's weight, are applied on the center of hip implant's head. McLeish and Chamley (1970) concluded on the results that for zero degree of pelvis angle, the direction of human body's force is approximately at 20° degrees to the center axis of femur bone. Finally, the magnitude of the force is depeneding on the weight of the human body and the type body movement. Bergmann (1993) proposed a percentage relationship between the type of movement and the weight of the human body. In Table 4, these percentage weight relations, depending on the type of movement, are listed as well as the nominal value of the force corresponding to an average body weight of 75 kg (Colica et. al., 2016).

Table 3. Loading of hip implant for different type of movement

Type of movement	Max. load (% weight)	Max. force on hip joint
Slow walking	282	2075 N
Climbing upstairs	356	2620 N
Climbing downstairs	387	2850 N
Tripping	720	5300 N

3. RESULTS AND DISCUSSION

3.1 Evaluation of solid hip implant

Before the topology optimization process occurs, it is necessary for the as-design product to be evaluated on its mechanical behavior through finite element analysis. Therefore, the 3D CAD model of solid hip implant (Figure 2) was examined as FEM under realistic *in vivo* conditions, as described in subsection 2.2. Figure 3 shows the contours of *von-Mises* stresses (Figure 3(a)) and the contours of the factor of safety (Figure 3(b)) for maximum load, i.e. at a force of 5300 N. These analyses extract a series of conclusions which are essential for the topology optimization process. The first deductible conclusion is that the head (ball) has low stress concentration, hence it receives small strains compared to the rest of the body. Furthermore, both the neck and the intramedullary stem are divided into three distinct regions of strain: the tensile region (left side), the low stresses region (center) and the compressive region (right side). In the tensile region, due to the direction

of the applied force, tensile stresses are concentrated, with the result that this region is a high-risk area for fracture. The central region of implant is also the area with the lowest stress concentration, where the improvement mass distribution is essential. Moreover, the compressive region is the area that again due to the direction of applied force, where there is concentration of compressive stresses and special treatment is needed to be taken during the process of topology optimization.

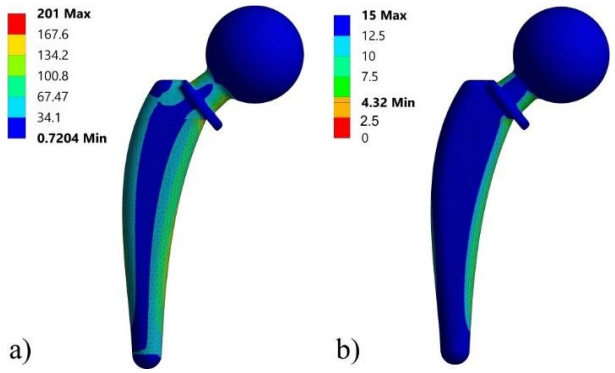

Fig. 3. a) Contour of *von-Mises* stresses; b) Contour of factor of safety (FOS)

As shown in Figure 3, the maximum stresses are compressive and they reach up to 201 MPa. However, these stresses are much lower than the material yield point, a conclusion that also results from the factor of safety (FOS) which has a minimum value of 4.32. Therefore, it could be concluded that the hip implant with this specific material and design withstands loads 4 times more than the maximum load that the implant receives from the human body, thus an extensive topology optimization of the design could be performed.

3.2 Topology optimization via lattice structures

In this section, the process of topology optimization of hip implant's design is analyzed using three different lattice structures, namely the octet strut-structure, the gyroid and the Schwarz diamond sheet-structures. The objective is to evaluate their mechanical behavior of each structure and to highlight the most advanced structure in order to promote them to the next phase of optimization, which is the adaptive adjustment of the lattice structure through functionally gradation. Topology optimization exploits the findings of the FEA of the previous subsection, hence that in certain areas the design is optimized. Having chosen the proper lattice structures, through the literature and their ability for stretching-dominated behavior, the next step is to select the appropriate relative density of the lattice structures region where redesign occurs. The appropriate value of the relative density should find the right tradeoff between the reduction of the mechanical properties due to size effect, and the desired advantages that the designer expects, i.e. reduction of the mass and increased porosity. Thus, the chosen relative density is 50%, due to the fact that it has a negligible influence from the size effect and this relative density is very close to the relative density of the femur bone (Thomas et. al., 1999), which enhances the body's ability to regenerate tissues.

The selection of redesigned regions with lattice structure is a result of FEA in the solid hip implant. Therefore, as illustrated in Figure 4, due to increased loads, both compressive and tensile in the neck of the implant, the whole area remains solid. The applied loads on the implant is occurred on the head, thus it is necessary to have a continuous solid surface of 2mm thickness, however because the head shows small stress concentration, hence its interior was redesigned with lattice structures, as shown in Figure 4. In addition, Figure 4 shows that the whole intramedullary stem is redesigned with lattice structure, exceptions are the region where the implant is beared, where it is remained solid, and the region where tensile stresses are concentrated which has been enhanced with a surface of 2mm thickness as the tensile strength of lattice structures is questionable.

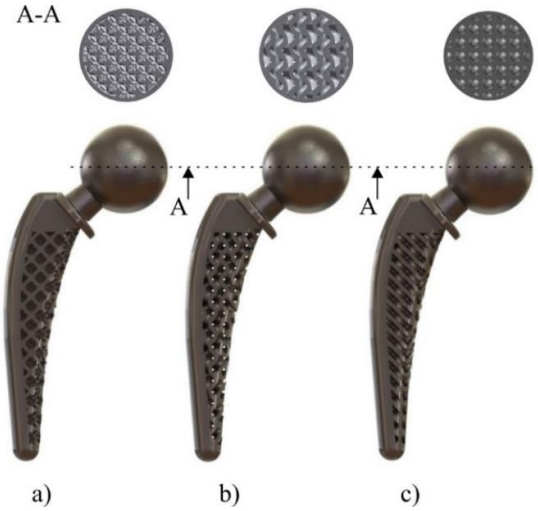

Fig. 4. Optimized hip implant designs via lattice structures: a) octet; b) gyroid; c) Schwarz diamond

Figure 5 shows the results of the finite element analysis for three different approaches of hip implant's topology optimization, using octet (Figure 5(a)), gyroid (Figure 5(b)) and Schwarz diamond (Figure 5(c)) structures, respectively. Specifically, according to Figure 5, the topology optimization approach, which has the highest strength, is the one that contains Schwarz diamond structure, followed by gyroid and octet structures, respectively. Hip implant which contain Schwarz diamond has the lowest stress concentration with maximum value of 780 MPa at compressive region. In addition, hip implant with gyroid structure shows a peak of compressive stresses at value of 930.2 MPa. Hip implant with octet structure is the weakest one with maximum stress concentration at 970.5 MPa.

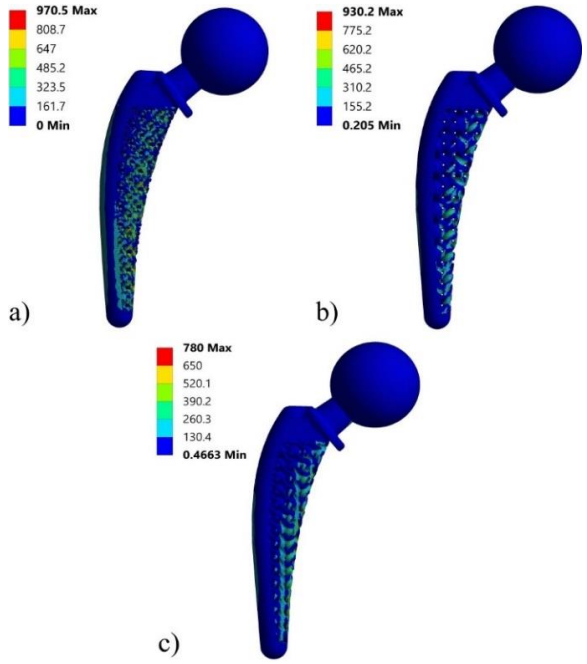

Fig. 5. Contour of *von-Mises* stress: a) octet structure; b) gyroid structure; c) Schwarz diamond structure

Having the values for the maximum stress concentration for each structure is easy to calculate the factor of safety, as listed in Table 5. In Table 5, in addition to the standard FOS, FOS_{Ult} is also calculated as the ultimate factor of safety and is depending on the ultimate strength of construction material. As FOS verifies, all three lattice structures could withstand the forces from the human body without fracture of the implant, as FOS_{Ult} is above than the one. However, the stress concentration in octet and gyroid structures is marginally greater than the yield point of the material, thus there may be occurred a plastic deformation of the object. On the other hand, the Schwarz diamond structure comfortably withstands the loads it receives, as the FOS reaches up to 1.17.

Table 4. Factor of safety for three different topology optimization approaches

Lattice structure	Factor of safety (FOS)	Ultimate factor of safety (FOS_{Ult})
Octet	0.94	1.13
Gyroid	0.98	1.18
S. diamond	1.17	1.41

4. CONCLUSIONS

In this study, an orthopedic hip implant was designed according to international standards, and then a topology optimization of its geometry was performed. The topology optimization was applied in the implementation of lattice structure in the proper regions, in order to achieve the optimal mass distribution within the existing volume. In particular, it seems that the hip implant, that contains Schwarz diamond structures, has the best mechanical behavior. This design approach shows a reduced weight of 36% compared to the solid version of hip implant, therefore less construction material is needed. Moreover, for the intramedullary stem it is valid that it has a 50% mean porosity to facilitate the process of tissue regeneration. Having the mechanical analysis, for topologically optimized hip implant, in a future study the fabrication of the redesigned hip implant could be done, through the process of additive manufacturing, and the examination of its mechanical behavior via the utility of proper experiments

5. REFERENCES

1. Al-Ketan, O., R. Rowshan, R. K. A. Al-Ruba, (2018). *Topology-Mechanical Property Relationship of 3D Printed Strut, Skeletal, and Sheet Based Periodic Metallic Cellular Materials*, Journal of Additive Manufacturing, 167-183.
2. Al-Ketan O., R. K. A. Al-Rub, (2019). *Multifunctional mechanical-metamaterials based on triply periodic minimal surface lattices: A review*, Journal of Advanced Engineering Materials, **21**(10), 1900524.
3. ASTM F2033-12, (2012). *Standard Specification for Total Hip Joint Prosthesis and Hip Endoprosthesis Bearing Surfaces Made of Metallic, Ceramic, and Polymeric Materials*, ASTM International, West Conshohocken, PA.
4. ASTM B348 / B348M-19, (2019). Standard Specification for Titanium and Titanium Alloy Bars and Billets, ASTM International, West Conshohocken, PA.
5. Bendsøe M. P., O. Sigmund, (2003). *Topology optimization: theory, methods, and applications*, Berlin; New York: Springer.
6. Bergmann, G., Graichen, F., Rohlmann, A., (1993). *Hip joint loading during walking and running, measured in two patients*, Journal of biomechanics, **26**(8), 969-990.
7. Boyer R., G. Welsch, E. W. Collings, (1994). *Materials Properties Handbook: Titanium Alloys*, ASM International, Materials Park, OH.
8. Charnley J., A. Kamangar, M. D. Longfield, (1969). *The optimum size of prosthetic heads in relation to wear of plastic sockets in total replacement of the hip*, Journal of Medical and Biological Engineering, **7**(1), 31–39.
9. Colica K., A. Sedmak, A. Grbovic, U. Tatic, S. Sedmak, B. Djordjevic, (2016). *Finite element modeling of hip implant static loading*, International Conference on Manufacturing Engineering and Materials, ICMEM, **149**, 257-262.
10. Ducheyne P., G. W. Hasting, (1984). *Functional behavior of orthopedic biomaterials*, Volume I:

Fundamentals, CRC Series in Structure-Property Relationships of Biomaterials.
11. Ehrgott M., (2005). *Multicriteria Optimization*, Berlin, Springer.
12. El-Shiekh H. El-Din F., (2002). *Finite Element Simulation of Hip Joint Replacement under Static and Dynamic Loading*, Ph.D. Thesis, School of Mechanical and Manufacturing Engineering Dublin City University.
13. España F. A., V. K. Balla, S. Bose, A. Bandyopadhyay, (2010). *Design and fabrication of CoCrMo alloy based novel structures for load bearing implants using laser engineered net shaping*, Journal of Material Science & Engineering C, **30**(1), 50-57.
14. Gabbrielli R., I. G. Turner, C. R. Bowen, H. Wang, S. Johnston, D. Rosen, A. Cheng, A. Humayun, D. J. Cohen, B. D. Boyan, (2006*). Design of a graded cellular structure for an acetabular hip replacement component*, Biofabrication.
15. Gebisa A. W., H. G. Lemu, (2017). *A case study on topology optimized design for additive Manufacturing*. IOP Conf. Ser.: Mater. Sci. Eng, **276**(1), 012026.
16. Gibson L. J., M. F. Ashby, (1997). *Cellular solids. Structure and properties*, Cambridge University Press.
17. González F. J. Q., (2016). *Computational Design of Functionally Graded Hip Implants by Means of Additively Manufactured Porous Materials*, Ph.D. Thesis, École de Technologie Supérieure, Montreal, QC, Canada.
18. González-Henríquez C. M., M. A. Sarabia-Vallejos, J. Rodriguez-Hernandez, (2019). *Polymers for additive manufacturing and 4D-printing: Materials, methodologies, and biomedical applications*, Journal of Polymer Science, Doi: 10.1016/j.progpolymsci.2019.03.001.
19. Hazlehurst K. B., C. J. Wang, M. Stanford, (2013). *The potential application of a Cobalt Chrome Molybdenum femoral stem with functionally graded orthotropic structures manufactured using Laser Melting technologies*, Journal of Medical Hypotheses, **81**(6), 1096-1099.
20. Heinl P., L. Muller, C. Korner, R. F. Singer, F. A. Muller, (2008). *Cellular Ti–6Al–4V structures with interconnected macro porosity for bone implants fabricated by selective electron beam melting*, J. of Acta Biomaterialia, doi: 10.1016/j.actbio.2008.03.013.
21. Helou M., S. Kara, (2018). *Design, analysis and manufacturing of lattice structures: an overview*, International Journal of Computer Integrated Manufacturing, 243-261.
22. Hybbinette C. H., (1985). *Long-term Results of Wear of Plastic Hip Prostheses*, Archives of Orthopaedic and Traumatic Surgery, **104**, 28–30.
23. Larsen S. D., O. Sigmund, J. P. Groen, (2018). *Optimal truss and frame design from projected homogenization-based topology optimization*, Journal of Structural Multidiscipline Optimization, **57**(4), 1461-1474.
24. Li C., I. Y. Kim, J. Jeswiet, (2015). *Conceptual and detailed design of an automotive engine cradle by using topology, shape, and size optimization*, Journal of Structural Multidiscipline Optimization, **51**, 547-564.
25. Limmahakhun S., A. Oloyede, N. Chantarapanich, (2017). *Alternative designs of load-Sharing cobalt chromium graded femoral stems*, Journal of Materials Today Communications, **12**, 1-10.
26. Mansour M., K. Tsongas, D. Tzetzis, A. Antoniadis, (2019). *The in-plane compression performance of hierarchical honeycomb additive manufactured structures*. IOP Conference Series: Materials Science and Engineering, **564**, 012015.
27. Mahmoud D., M. A. Elbestawi, (2017). *Lattice Structures and Functionally Graded Materials Applications in Additive Manufacturing of Orthopaedic Implants: A Review*, Journal of Manufacturing and Materials Processing, **1**(2), 13, https://doi.org/10.3390/jmmp1020013.
28. McKee G. K., (1967). *Development in total hip joint replacement*, Proceedings of the Institution of Mechanical Engineers, **181**, 85-89.
29. McLeish R. D., J. Chamley, (1970). *Abduction forces in the one-legged stance*, Journal of Biomechanics, doi: 10.1016/0021-9290(70)90006-0.
30. Müller M. E., (1970). *Total hip prosthesis*, Journal of Clinical Orthopaedics and Related Research, **72**, 46-68.
31. Rosen D. W., (2014). *Research supporting principles for design for additive manufacturing*, Journal of Virtual and Physical Prototyping, 225-232.
32. Thomas C. D. L., S. A. Feik, J. G. Clement, (1999). *Regional variation of intracortical porosity in the midshaft of the human femur: age and sex differences*, Journal of Anatomy, **206**(2), 115-25.
33. Tyflopoulos E., D. T. Flem, M. Steinert, A. Olsen. (2018). *State of the art of generative design and topology optimization and potential research needs*. Proceedings of NordDesign 2018, Linköping, Sweden, ISBN: 978-91-7685-185-2.

Received: April 24, 2020 / Accepted: December 20, 2020 / Paper available online: December 25, 2020